Photometric and spectroscopic evolution of type II-P supernova SN 2004A

Uday K. Gurugubelli[1,2], D. K. Sahu[2], G. C. Anupama[2] and
N. K. Chakradhari[2]

[1] *Joint Astronomy Programme, Indian Institute of Science, Bangalore, India*
[2] *Indian Institute of Astrophysics, Bangalore, India*

Abstract. We present optical photometry and spectroscopy of the normal type IIP supernova SN2004A, which was discovered in the galaxy NGC 6207 on 2004 January 9.84UT. Early observations indicated that the supernova was discovered at about two weeks since explosion. We estimate the distance to NGC 6207 to be 20.35±4.5 Mpc using the Standard Candle method. Using this distance, we estimate the ejected nickel mass in the explosion to be 0.032±0.02 $M_\odot$. The plateau luminosity, its duration (about 80 days) and the expansion velocity of the supernova ejecta at the middle of the plateau indicate an explosion energy of $4.7 \pm 2.7 \times 10^{50}$ ergs and an ejected envelope mass of 7.2± 2.2 $M_\odot$. The ejected envelope mass implies a main sequence mass of 10± 2.5$M_\odot$ for the progenitor.

Keywords : stars: evolution – supernovae: general – supernovae: individual: SN 2004A – galaxies: individual: NGC 6207 – galaxies: distances and redshifts

1. Introduction

Core-collapse supernovae (CCSNe), which includes supernovae of all other types except the thermonuclear type Ia events, are thought to emerge from the shock driven explosion of massive (M > 8$M_\odot$) stars (Woosley & Weaver 1986). Most of the observed differences in the properties of various subclasses of the CCSNe, namely type IIP, IIL, Ib, Ic, IIn can be explained by the ability of the SN progenitor to retain their hydrogen/helium rich envelope prior to explosion, the density of the medium in which they explode, mass loss history of the progenitor, metallicity and rotation of the progenitor (Heger et al. 2003; Hamuy 2003).

Type IIP supernovae are characterized by a long plateau in their light curve during which the brightness remains within ~ 1 mag of the maximum brightness for few months, followed by a steep decline and a quasi exponential tail in the later stage. The long plateau can be attributed to the moving hydrogen recombination wave in the thick massive envelope of the progenitor star, which was initially ionized because of the energy deposited by the shock wave and radio active decay. The quasi exponential decay in the later stage is explained by the instant reprocessing of the energy of radio active decay of ^{56}Co to ^{56}Fe.

Type IIP supernovae are gaining further importance because of their use as distance indicators. They are the most common type of supernova and more abundant per unit volume (Mannucci et al. 2005; Cappellaro et al. 2005). The expanding photosphere method (EPM) provides a way to estimate the distance of the host galaxy (Krishner & Kwan 1974; Schmidt et al. 1994). Hamuy & Pinto (2002) demonstrated that the EPM can be replaced by a more practical empirical method, known as standard candle method (SCM), which requires less input data. After incorporating the refinements related to the extinction corrections, Nugent et al. (2006) have shown that the practicality of measuring distances using SCM at cosmological redshift, has significantly improved. Thus SNe IIP can also serve as an independent and perhaps absolute distance indicator.

SN 2004A was discovered on January 9.84 UT and later confirmed on January 10.75 UT by K. Itagaki (IAUC 8265), around $22''$ west and $17''$ north of the centre of a nearby spiral galaxy NGC 6207. Optical spectra taken on January 11.8 and 11.9 showed blue continuum and hydrogen Balmer lines with P-Cygni profiles (Kawakita & Kinugasa 2004). The observed blue continuum and weak emission features suggested that the SN was discovered young. The expansion velocity, measured from the minima of the Balmer lines, was around $12\,000\,\mathrm{km\,s^{-1}}$.

The photometric studies of SN 2004A carried out by Hendry et al. (2006) showed that it was a normal type IIP supernova discovered about two weeks after the explosion. A mean distance of 20.3±3.4 Mpc for the host galaxy and $0.046^{+0.031}_{-0.017}$ M$_\odot$ of ejected ^{56}Ni during the explosion have been estimated. The search for progenitor in the archival pre-explosion HST WFPC2 images led Hendry et al. (2006) to identify the progenitor as a star with a magnitude $m_{\mathrm{F814W}} = 24.3 \pm 0.3$, which was likely to be a red supergiant with a mass of 9^{+3}_{-2} M$_\odot$.

In this paper photometric and spectroscopic studies of SN 2004A are presented. The photometric and spectroscopic data are presented in Section 2 and Section 3, respectively. The data are analyzed in Section 4. The distance of the host galaxy NGC 6207, using the refined Standard Candle Method is estimated in Section 5. Mass of ^{56}Ni ejected during the explosion and the properties of the progenitor have been estimated in Section 6 and Section 7, respectively.

Table 1. List of Landolt standard fields used for calibration.

Date	Standard fields
2004 Mar 10	PG0918+029, PG0942–029, PG1047+003, PG1323–086, PG1530+057
2004 May 11	PG1633+099, PG1657+078, SA113, SA107
2004 May 13	PG1530+057, PG1525–071, PG1407–013, PG1528+062, PG1633+099

2. Photometry

2.1 Observations and data reduction

Supernova SN 2004A was monitored in BVRI bands with 2.0 m Himalayan Chandra Telescope (HCT) of the Indian Astronomical Observatory (IAO), Hanle, India, using the Himalaya Faint Object Spectrograph Camera (HFOSC) equipped with 2048×4096 pixel CCD. The central 2048×2048 region of the CCD, which covers a field of view of 10×10 arcmin, with a plate scale of 0.296 arcsec pixel^{-1}, was used for imaging. The photometric monitoring of SN 2004A began on 2004 January 27 and continued until 2004 September 06. Photometric standard star fields (Landolt 1992) listed in Table 1 were observed during photometric nights to calibrate a sequence of secondary standards in the supernova field using the following transformation equations:

$$u = U - (0.188 \pm 0.012)(U - B) - 3.233 \pm 0.011$$
$$b = B + (0.076 \pm 0.022)(B - V) - 1.076 \pm 0.021$$
$$v = V - (0.043 \pm 0.014)(B - V) - 0.701 \pm 0.013$$
$$r = R - (0.073 \pm 0.032)(V - R) - 0.772 \pm 0.012$$
$$i = I - (0.045 \pm 0.015)(V - I) - 1.044 \pm 0.011$$

The data reduction was done in a standard manner using various tasks available within *IRAF*[1]. The data were bias subtracted, flat-field corrected using twilight sky flats and cosmic rays removed. Aperture photometry was performed on the standard star fields observed during photometric nights and a set of stars in the supernova field, marked in Figure 1, were calibrated. The calibrated magnitudes of the secondary standard in the supernova field averaged over three nights are given in Table 2. These magnitudes were then used to calibrate the data obtained on other nights.

In order to minimize the effects of variation in the galaxy background at the location

---

[1]*IRAF* is a data reduction software, distributed by the National Optical Astronomy Observatory.
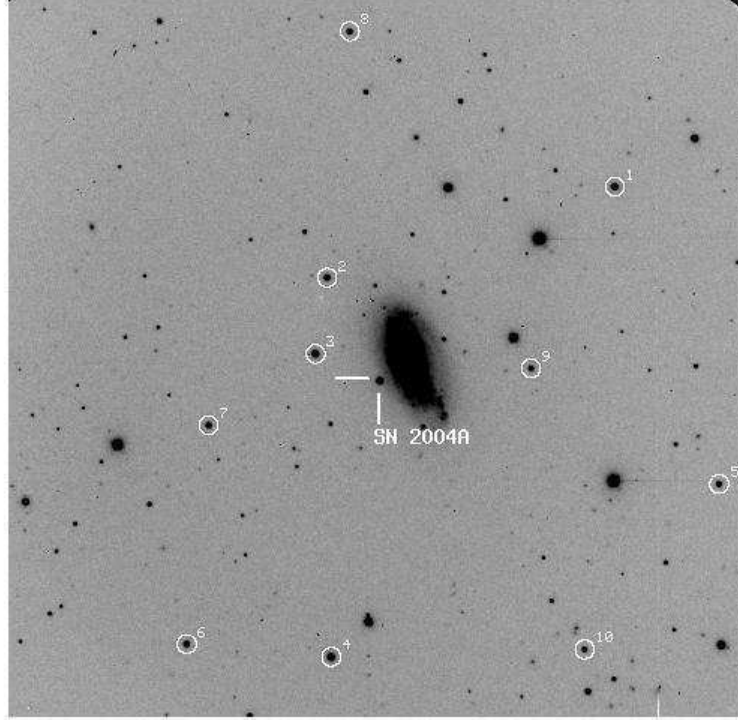
Figure 1. Finder chart for SN 2004A. The stars labeled by numbers are used as local standards to calibrate the supernova.

of supernova, the instrumental magnitudes of supernova were determined using the point spread function (PSF) fitting technique, with a fitting radius similar to the FWHM of the seeing profile. The magnitudes of the local standards were extracted using aperture photometry with aperture of radius 3-4 times that of the FWHM. The difference between the aperture and profile fitting photometry was estimated using the bright local standards in the field and applied to the supernova magnitude. Typical value of the correction applied to the R band PSF magnitude is of the order of 0.35 mag. Finally, the instrumental magnitudes of the supernova were calibrated differentially using the secondary standards. The estimated supernova magnitudes and the seeing in R band are reported in Table 3.

2.2   Light curves

The light curves of SN 2004A in $BVRI$ bands are shown in Figure 2. From the light curves it is apparent that the supernova exhibits a distinct plateau lasting until about

Table 2. Photometry of stars in the field of SN 2004A. The stars are labeled in the same way as in Fig. 1.

Star ID	B	V	R	I
1	15.85(0.004)	15.24(0.019)	14.88(0.005)	14.49(0.03)
2	16.45(0.006)	15.66(0.028)	15.28(0.002)	14.88(0.02)
3	16.08(0.002)	15.24(0.021)	14.81(0.002)	14.37(0.01)
4	15.67(0.017)	15.03(0.021)	14.67(0.012)	14.31(0.02)
5	16.76(0.002)	16.08(0.014)	15.71(0.012)	15.31(0.02)
6	16.73(0.023)	15.95(0.020)	15.52(0.015)	15.08(0.01)
7	16.68(0.010)	16.01(0.026)	15.65(0.008)	15.25(0.02)
8	16.64(0.005)	16.01(0.031)	15.66(0.000)	15.28(0.03)
9	17.08(0.000)	16.40(0.014)	16.05(0.006)	15.68(0.02)
10	17.23(0.003)	16.52(0.009)	16.12(0.004)	15.72(0.01)

80 days since explosion. During the plateau, V, R and I bands show a nearly constant brightness, whereas the B band light curve declines steeply with a decline rate $\beta^B_{100} \sim$ 2.0 mag, firmly establishing that SN 2004A is a Type IIP event (Patat et al. 1994).

After the plateau phase there is a steep decline in the brightness of the supernova in all bands, marking the transition from the photospheric phase to the nebular phase. The light curve declines by 2, 2, 1.8, and 1.6 mag in $BVRI$ bands during this transition period, from days 90 to 130. Beyond day 130, during the late phase, the light curves decline linearly in all bands with a decline rate of $\gamma_B \sim 0.01$ mag day^{-1}. The photometric evolution of type IIP SNe at late phases is powered by radioactive decay of ^{56}Co into ^{56}Fe, and the expected decay rate is 0.98 mag $(100d)^{-1}$, especially in the V band. The decay rates obtained during the late phase are close to the expected rate for ^{56}Co $\rightarrow$ ^{56}Fe decay, suggesting an efficient γ-ray trapping.

A comparison of the light curves of SN 2004A with those of the well studied type IIP SNe SN 2004et (Sahu et al. 2006) and SN 1999em (Leonard et al. 2002) is made. Light curves of SN 2004A are plotted in Fig. 2 along with the light curves of SN 2004et and SN 1999em. The $BVRI$ light curves of SN 1999em and SN 2004et have been shifted arbitrarily in magnitudes to match the light curves of SN 2004A.

The length of the plateau is 80d for SN 2004A, 110d for SN 2004et (Sahu et al. 2006) and 95d for SN 1999em (Leonard et al. 2002). The overlap of the $BVRI$ light curves of the three SNe is fairly good during plateau phase, while some differences are visible during the late phase. The slopes of the V, I light curves of all three SNe are the same, while SN 2004A is brighter than SN 2004et and comparable to SN 1999em.

The reddening corrected $B - V$, $V - R$, $R - I$, $V - I$ colour curves of SN 2004A are shown in Fig. 3. Also shown in the same figure are the respective colour curves

Table 3. Journal and results of optical photometry of SN 2004A.

JD (245 3000+)	*Phase (days)	B	V	R	I	seeing (arcsec)
031.53	21	–	15.55(0.01)	15.15(0.01)	14.77(0.04)	1.9
036.50	26	16.16(0.01)	15.57(0.01)	15.17(0.01)	14.92(0.01)	2.3
044.46	34	16.29(0.02)	15.57(0.02)	15.16(0.03)	14.85(0.04)	2.3
051.45	41	16.41(0.01)	15.55(0.02)	15.13(0.01)	14.80(0.01)	2.1
064.48	54	16.59(0.01)	15.56(0.02)	15.09(0.02)	14.78(0.01)	1.9
065.43	55	16.57(0.01)	15.55(0.01)	15.10(0.02)	14.74(0.02)	2.3
075.49	65	16.65(0.01)	15.55(0.01)	15.07(0.01)	14.74(0.01)	2.1
081.34	71	16.70(0.01)	15.56(0.01)	15.09(0.01)	14.75(0.01)	1.4
099.35	89	16.89(0.02)	15.68(0.01)	15.19(0.01)	14.85(0.01)	1.6
102.41	92	16.93(0.02)	15.73(0.03)	15.23(0.02)	14.88(0.01)	1.5
110.30	100	17.14(0.01)	15.86(0.01)	15.36(0.01)	15.00(0.01)	1.8
119.33	109	17.48(0.04)	16.14(0.02)	15.62(0.02)	–	1.5
124.38	114	–	–	15.93(0.01)	–	1.9
125.31	115	18.10(0.01)	16.58(0.02)	16.00(0.01)	15.57(0.03)	2.7
129.31	119	18.60(0.01)	16.99(0.02)	16.33(0.01)	15.88(0.02)	1.9
131.28	121	18.75(0.02)	17.18(0.02)	16.50(0.02)	16.05(0.02)	1.5
133.39	123	–	17.36(0.01)	16.67(0.03)	16.22(0.02)	2.0
135.43	125	19.09(0.02)	17.44(0.01)	16.74(0.01)	16.26(0.02)	1.7
137.36	127	19.16(0.02)	17.06(0.09)	16.77(0.01)	16.30(0.01)	2.1
138.32	128	–	–	16.78(0.01)	16.28(0.01)	2.1
139.43	129	19.12(0.02)	17.49(0.01)	16.80(0.01)	16.32(0.01)	1.5
146.26	136	–	17.58(0.01)	16.85(0.01)	16.40(0.02)	1.9
157.38	147	19.34(0.01)	17.69(0.01)	16.95(0.01)	16.52(0.01)	2.0
159.29	149	–	–	16.97(0.02)	16.50(0.01)	1.9
170.22	160	19.32(0.02)	17.82(0.01)	17.07(0.01)	16.61(0.01)	1.4
185.18	175	–	17.96(0.01)	17.20(0.02)	16.76(0.01)	1.3
187.27	177	19.59(0.03)	18.00(0.02)	17.21(0.02)	16.77(0.01)	1.5
202.14	192	19.59(0.01)	18.17(0.01)	17.32(0.02)	16.92(0.01)	1.7
206.12	196	19.65(0.02)	18.23(0.01)	17.35(0.01)	16.94(0.01)	1.8
216.25	206	19.71(0.02)	18.29(0.01)	17.44(0.01)	17.02(0.01)	1.5
223.31	213	19.82(0.03)	18.45(0.01)	17.51(0.01)	17.13(0.01)	1.6
225.19	215	19.81(0.01)	18.44(0.01)	17.51(0.01)	17.13(0.01)	1.7
228.15	218	19.84(0.01)	18.46(0.01)	17.54(0.01)	17.18(0.01)	1.7
229.14	219	19.79(0.02)	18.47(0.01)	17.55(0.01)	17.15(0.02)	1.8
231.11	221	–	–	17.58(0.02)	–	1.2
233.19	223	19.81(0.01)	18.53(0.01)	17.58(0.01)	17.26(0.01)	1.5
245.23	235	20.07(0.03)	18.69(0.02)	17.68(0.03)	17.31(0.01)	2.0
246.19	236	20.09(0.03)	18.67(0.02)	17.70(0.02)	17.35(0.01)	2.1
255.07	245	–	18.74(0.02)	17.76(0.02)	17.47(0.03)	1.5

∗ Relative to the epoch of date of explosion(JD = 245 3010)

NOTE: Figures in brackets give the statistical errors associated with the magnitudes.
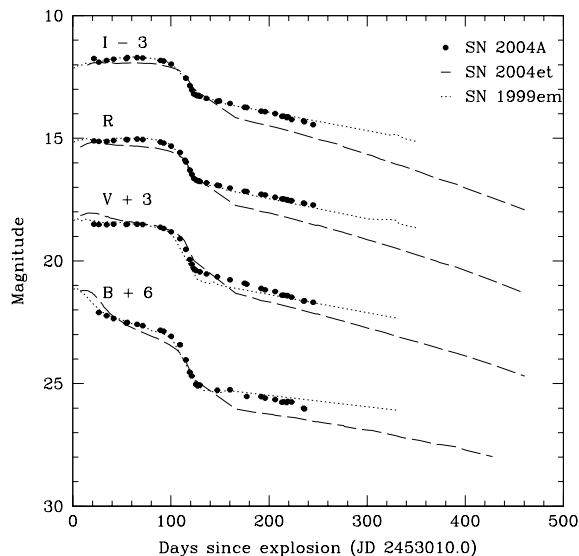
Figure 2. BVRI light curves of SN 2004A plotted with other type II-P SNe. Light curves of SN 2004A have been shifted by the reported amounts, other light curves have been shifted arbitrarily to match those of SN 2004A.

of SN 1999em and SN 2004et. Colour curves of SN 1999em and SN 2004et have been corrected for colour excess using $E(B-V) = 0.1$ and 0.45 respectively; and the Cardelli et al. (1989) interstellar extinction law. The colour evolution of SN2004A in $B-V$ is very similar to that of the other two supernovae. The $V-R$ colour evolution of SN2004A is similar to that of SN2004et and SN1999em until day 200, beyond which SN 2004A trends redward while the other two SNe show a blueward trend. In the $R-I$, SN 2004A evolves similar to SN 1999em until day 150, beyond which SN 2004A colours are bluer than SN 1999em. On the other hand, SN 2004et remains bluer than both SN 2004A and SN 1999em throughout. A similar trend is seen in the $V-I$ colour evolution also.

3. Spectroscopy

3.1 Observations and data reduction

The journal of spectroscopic observations of SN 2004A is given in Table 4. The spectroscopic observations began on Feb 28, 2004 and continued until June 30, 2004. All spectra were obtained in the wavelength range 3500–7000 Å and 5200–9200 Å, at a spectral resolution of ~ 7 Å and spectra were reduced in a standard manner, using various available tasks within IRAF. The frames were debiased, and flat-field corrected. One dimensional
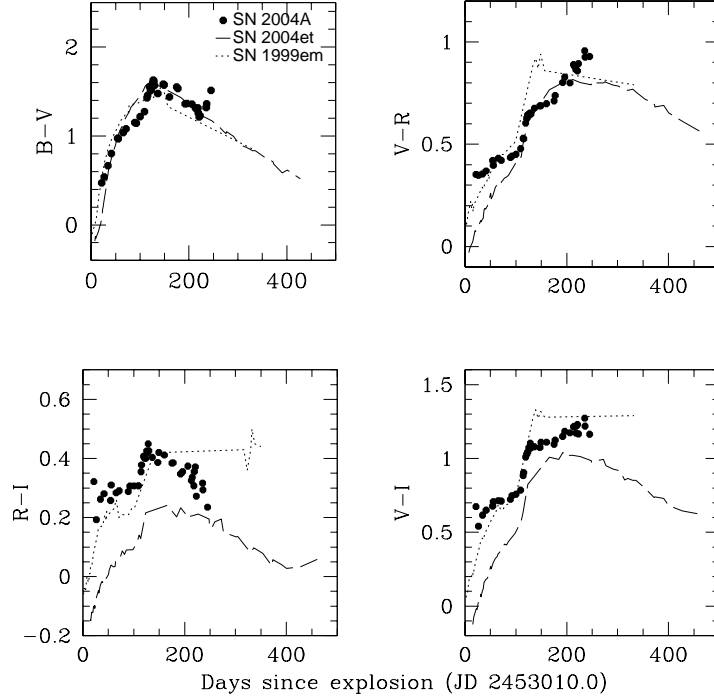
Figure 3. Colour curves of SN 2004A compared with other SNe.

spectra were extracted from the two dimensional images using the optimal extraction method (Horne 1986). Arc lamp spectrum of FeAr and FeNe were used for wavelength calibration. Accuracy of wavelength calibration was checked by determining the position of the night sky lines. The spectra were then flux calibrated using the instrumental response curve generated using the spectrophotometric flux standards observed on the same night with the same instrumental setup. On a few nights when the spectrophotometric standards were not observed, the response curves obtained on other nearby nights were used for flux calibration. The flux calibrated spectra in two regions were combined to a weighted mean to give the final spectrum. The spectra were brought to an absolute flux scale using zero points obtained by comparing with the photometric magnitudes. The telluric lines have not been removed from the spectra.

3.2 Spectroscopic evolution

The spectroscopic evolution of SN 2004A is displayed in Figs 4 and 5 and the lines are identified in Fig. 6. The spectra have been corrected for the redshift of the parent galaxy

Table 4. Journal of spectroscopic observations of SN 2004A.

Date	JD (245 0000+)	*Phase (days)	Wavelength Range (Å)
2004 Feb 28	3064.5	54	3500−7000; 5200−9200
2004 Feb 29	3065.5	55	3500−7000; 5200−9200
2004 Mar 13	3078.5	68	3500−7000; 5200−9200
2004 Mar 25	3090.5	80	5200−9200
2004 Apr 03	3099.5	89	3500−7000; 5200−9200
2004 Apr 25	3121.5	111	3500−7000; 5200−9200
2004 May 05	3131.5	121	5200−9200
2004 May 08	3134.5	124	3500−7000; 5200−9200
2004 May 26	3152.5	142	3500−7000; 5200−9200
2004 May 31	3157.5	147	3500−7000; 5200−9200
2004 Jun 13	3170.5	160	3500−7000; 5200−9200
2004 Jun 23	3180.5	170	3500−7000; 5200−9200
2004 Jun 28	3185.5	175	3500−7000; 5200−9200
2004 Jun 30	3187.5	177	3500−7000; 5200−9200

*Relative to the epoch explosion (JD = 2453010).

NGC 6207 and not for reddening. Our first spectrum is taken ~ 54 days after explosion, which corresponds to almost the middle of the plateau. At this epoch the spectrum is dominated by strong lines of H with well developed P-Cygni profiles. Numerous other lines due to CaII (H & K and NIR triplet), FeII, NaI, ScII, CaII, BaII have also been identified in the spectrum (Leonard et al. 2002).

Hα line emission show a strong P-Cygni profile, which appears to consist of two components. A similar feature is associated with Hβ also, which is seen until ~ 110 days after explosion. Baron et al. (2000) coined the term 'complicated P-Cygni profile' to explain the double P-Cygni absorption as a combination of the usual wide P-Cygni profile and a second P-Cygni profile with a highly blue-shifted absorption, corresponding to two line forming regions in the expanding atmosphere of the supernova, which could arise either by an unusual density structure of the progenitor star or by strong mixing and asphericity of the ejecta. The complicated P-Cygni profile is already reported in SN 1999em (Baron et al. 2000; Leonard et al. 2002), SN 2004et (Sahu et al. 2006), and SN 2005cs (Pastorello et al. 2006). The absorption on the blue side of Hα and Hβ lines appears to be much stronger in SN 2004A as compared to other type IIP SNe. The absorption on the blue side of Hα and Hβ lines could be due to either high-velocity features of H lines or absorption lines of N II (λ 4623) and Si II (λ 6355) ions. Based on the velocity estimates of the absorption lines, Pastorello et al. (2006) have shown that the absorption in the blue wing of Hβ line could be due to NII and that of Hα line could
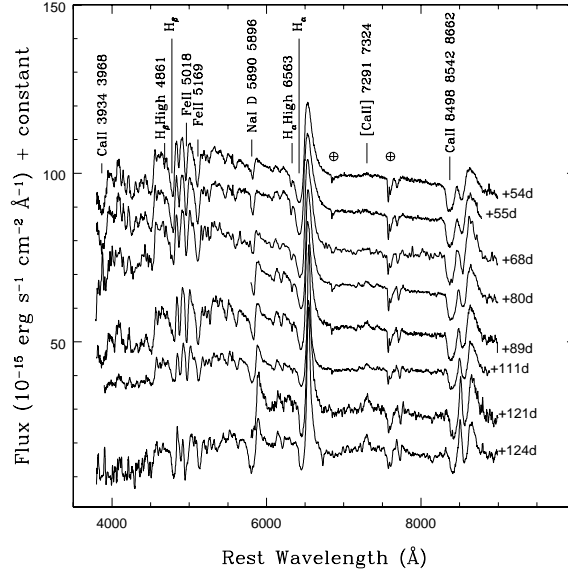
Figure 4. Spectroscopic evolution of SN2004A during the plateau phase.

be due to Si II. However, the consistency of the measured velocities of Hα and Hβ in SN 2004A shows that they are most likely due to the high velocity components.

As the supernova ages, the absorption components of Hα, Hβ and the CaII IR triplet become narrower and deeper. In the blue region of the spectrum numerous metal lines due to Fe, Sc, Ba and Sr appear and the emission line strength increases with time till the supernova enters into the nebular phase.

The spectra during days 140 to 170 (Fig. 5) show permitted lines due to metals. The P-Cygni profiles gradually fade during this period and narrow forbidden emission lines [O I] 6300, 6364 Å and [Ca II] 7291, 7324 Å start appearing in the spectrum, indicating the onset of nebular phase. The lack of prominent forbidden lines in the spectra indicates that the supernova was not completely transformed into nebular phase.

3.3 Expansion velocity

The velocity evolution of various spectral lines in SN 2004A is presented in Fig. 7. The expansion velocities were measured from the minimum of the blue-shifted absorption trough of the Fe II 4924, 5018, 5169 and H$_\alpha$, H$_\beta$. The velocities have been corrected for the recession velocity of 852 km s^{-1} for NGC 6207 (Haynes et al. 1998). The expansion ve-
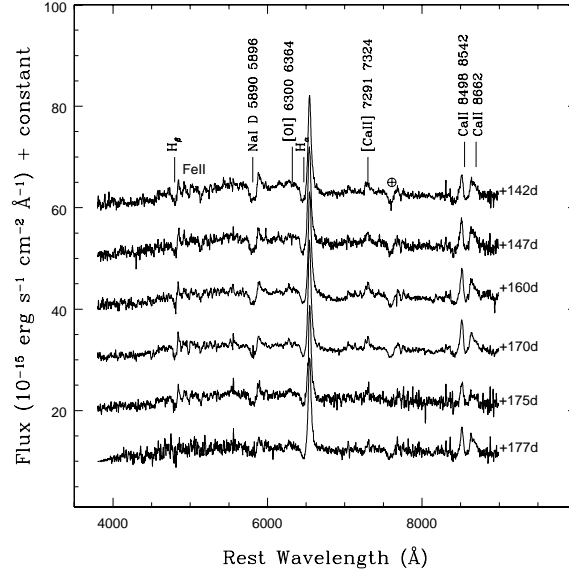
Figure 5. Spectroscopic evolution of SN2004A during the late phase.
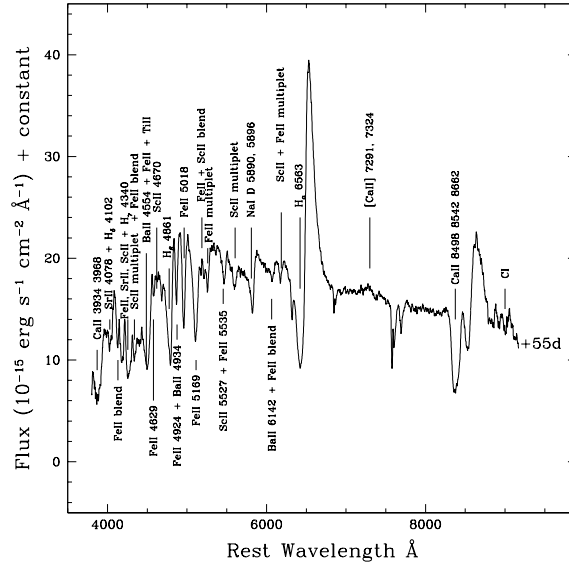

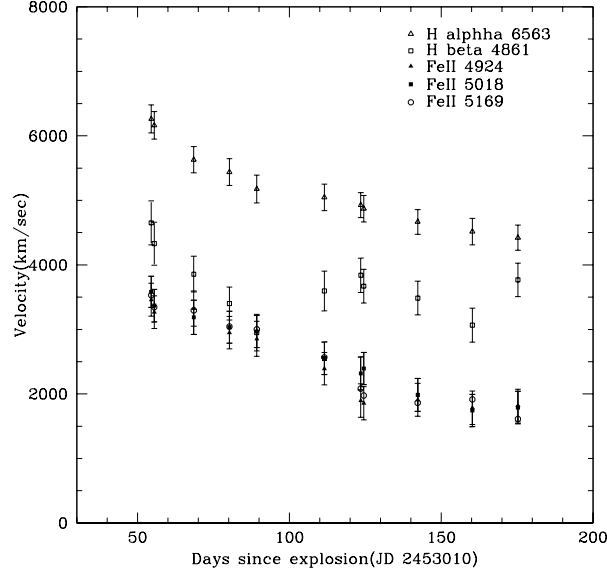**Figure 6.** Line identification during middle of the plateau.

Figure 7. Velocity evolution of SN 2004A.

locity measured using different species declines slowly with time. The velocity estimates, derived from H_α, H_β lines are always higher in comparison to those estimated using Fe II (λ4924, 5018, 5169). It is because they are formed at the top of the photosphere and have higher optical depths. However, the velocities derived using the Fe II λ4924, 5018, 5169 lines are supposed to be a good estimate of the photospheric expansion velocity, as they are formed close to the photosphere and are weak and unblended (Eastman & Krishner 1989).

The expansion velocity of the high velocity component of H_α and H_β is also plotted in Fig. 7. The estimated velocity of these lines are consistent with each other, indicating that they are formed in the same high velocity region, and the evolution of these lines are very similar to those of other lines namely H_α, H_β and multiplets of FeII, with almost constant offset of 4500 $km\,s^{-1}$.

4.　Estimation of explosion epoch and reddening

4.1　Explosion epoch

An estimate of the explosion epoch is made by comparing the light curve of SN 2004A with those of SN 1999em (Leonard et al. 2002). Time and apparent magnitudes of the light curves of SN 1999em are adjusted to get the best match to the data points
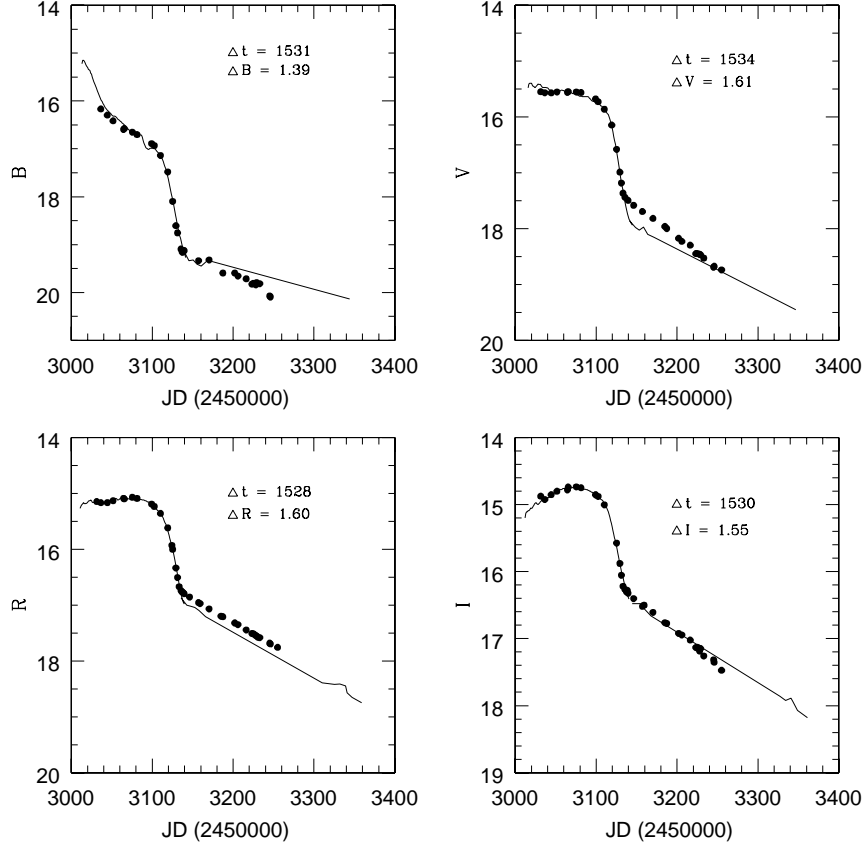
Figure 8. *BVRI* light curves of SN 2004A (filled circles), over-plotted with the best fit light curve of SN 1999em, (solid line), shifted by Δt days and Δm magnitudes.

of SN 2004A, by minimizing the χ^2. The data points covering the plateau and the transition to nebular phase have been considered for comparison. The offsets in time Δt and apparent magnitudes Δm between SN 1999em and SN 2004A for each bands have been listed in Table 5. The shifted light curves of SN 1999em in $BVRI$ bands have been over plotted with the observed points of SN 2004A in Fig. 8. The explosion epoch of SN 1999em is well constrained by Hamuy et al. (2001) as JD 2451478.8±0.5. Using this and the average offset of 1531 days in explosion epoch between SN 1999em and SN 2004A the explosion epoch of SN 2004A has been estimated as JD 245 3010 ± 2.5, which corresponds to January 5, 2004. The error in the explosion epoch is estimated from the error in the weighted average of Δt.

Table 5. Results from the least-square fitting algorithm which adjusts the time Δt, and apparent magnitude Δm, of the 'model' light curve (SN 1999em) to find the best fit to the data points of SN 2004A.

Filter	Δm (days)	Δt (JD 245 0000)	explosion epoch
B	1.39(0.05)	1531(2)	3010(2)
V	1.61(0.02)	1534(2)	3013(2)
R	1.60(0.01)	1528(2)	3007(2)
I	1.55(0.01)	1530(2)	3009(2)
$BVRI$		1531(2)	3010(2)

4.2   Reddening estimation

The Galactic reddening in the direction of NGC 6207 is $E(B-V)_G = 0.015$ mag (Schlegel, Finkbeiner & Davis 1998). In the spectrum taken on Feb. 28, 2004, the interstellar NaID line is seen clearly with an equivalent width of 0.4Å, which corresponds to a total reddening of $E(B-V) = 0.10$, following the calibration by Munari & Zwitter (1997). For a sample of type Ia supernovae, Turatto, Benetti & Cappellaro (2003) have shown that the relation between equivalent width and reddening is bivariate with most of the less reddened objects following the relation $E(B-V) = 0.16 \times EW(NaID)$. This relation gives an estimate of reddening as $E(B-V) = 0.06$ towards SN 2004A, which is consistent with the estimate by Hendry et al. (2006) using the neighboring stars. The reddening corrected colours of SN 2004A are similar to those of SN 1999em, indicating that the derived colour excess towards SN 2004A is consistent with the intrinsic colours of type IIP SNe as all type IIP SNe are supposed to attain similar intrinsic colour towards the end of plateau (Eastman, Schmidt & Kirshner 1996).

5.   Distance estimation

The Standard Candle Method (SCM), to estimate distance of type IIP SNe is based on the correlation between the expansion velocities of the ejecta and their bolometric luminosity during the plateau phase. This was first formulated by Hamuy & Pinto (2002) and later Hamuy (2004) calibrated the Hubble diagram using a sample of 24 SN IIP, with known Cepheid distances to four of these SNe. This method has recently been refined by Nungent et al. (2006) by introducing the use of $(V - I)$ colours during the plateau phase, at day 50, to perform extinction correction rather than relying on colours at the end of the plateau.

We used equations (5) and (6) from Hamuy (2004) to estimate the distance to SN 2004A. The V, I magnitudes and expansion velocity of SN2004A for phase 54 day are

available from our observations. We have linearly extrapolated the expansion velocity and interpolated the magnitudes to day 50. The interpolated magnitudes for phase 50 day are $V_{50} = 15.55 \pm 0.02$ mag and $I_{50} = 14.77 \pm 0.01$ mag, and the expansion velocity at this phase is $v_{50} = 3266.0 \pm 225.0$ km sec^{-1}. Using these magnitudes, expansion velocity and the reddening determined in Section 4.2, distance to supernova SN 2004A is estimated as D(V) = 20.16 ± 3.54 Mpc and D(I) = 20.54 ± 2.91 Mpc. Using the refinement of SCM method by Nugent et al. (2006) the distance is estimated as 20.51 ± 1.25 Mpc, in good agreement with the earlier estimate. A straight average of these results gives a distance of D = $20.35^{+3.35}_{-3.73}$ Mpc, where the errors are estimated from the limits of D(V) and D(I). The average distance of SN 2004A estimated using the standard candle method compares very well with the mean distance of 20.3 ± 3.4 Mpc by Hendry et al. (2006), which is arrived at using three different methods namely the standard candle method, brightest supergiant distance using HST photometry and the kinematic distance available in the literature.

6.   Estimation of ejected Ni mass

6.1   Bolometric light curve

The reddening and distance estimates obtained in the previous sections, along with the $BVRI$ photometric data is used to compute the bolometric light curve of SN 2004A. The missing magnitudes in some bands were obtained by interpolating between points adjacent in time. The optical magnitudes have been corrected for reddening $E(B - V) = 0.06$ using interstellar extinction law (Cardelli et al. 1989). The emitted flux is estimated by converting the corrected magnitudes into flux according to Bessell et al. (1998). The $BVRI$ fluxes were derived by fitting spline curve to the B, V, R and I fluxes and integrating it over the wavelength range 3600–10600 Å. Unfortunately, U band magnitudes of supernova were not avilable. The contribution of U flux to the $UBVRI$ bolometric flux was determined using supernovae SN 1999em and SN 2004et, and the same fraction is added to the $BVRI$ flux of SN 2004A to get the $UBVRI$ bolometric flux. No corrections have been applied for the missing flux in UV and IR bands. The bolometric light curve of SN 2004A is plotted in Fig. 9. For the purpose of comparison the bolometric light curves of SN 2004et (Sahu et al. 2006) and SN 1999em (Leonard et al. 2002; Elmhamdi et al. 2003b) and SN 1987A (Suntzeff & Bouchet 1990) have also been plotted in the same figure. The bolometric light curve evolution of SN 2004A is very similar to SN 2004et and SN 1999em. At all epochs the bolometric luminosity of SN 2004A is intermediate between the luminous SN 2004et and normal SN 1999em, it is marginally brighter than SN 1999em.

6.2   Nickel mass from bolometric luminosity of exponential tail

The lightcurve of supernovae in the nebular phase is powered by the radioactive decay of ^{56}Co to ^{56}Fe, which is a daughter nuclei of ^{56}Ni. Thus the bolometric luminosity in the nebular phase of type IIP supernovae can be used to estimate the amount of ^{56}Ni freshly
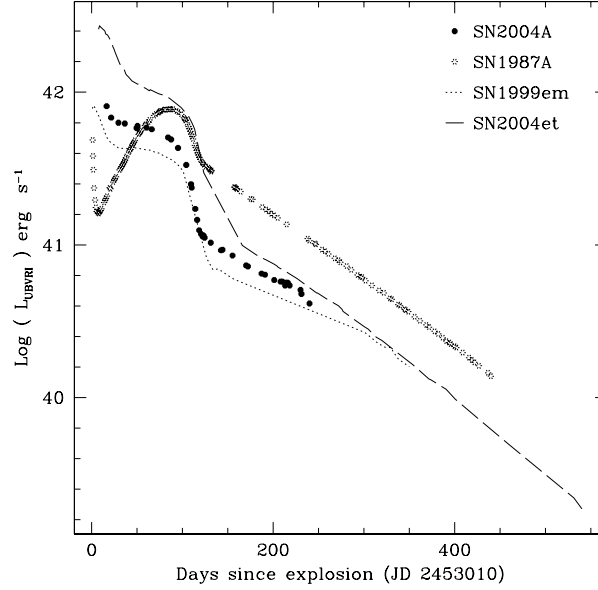
Figure 9. Bolometric light curve of SN 2004A.

synthesized during the explosion. The bolometric luminosity of the exponential tail for a sample of type IIP supernovae was used to estimate the mass of ^{56}Ni assuming that all of the γ-rays resulting from the ^{56}Co to ^{56}Fe decay are fully thermalised. The mass of ^{56}Ni produced during the explosion of type IIP supernovae vary by a factor of ~ 100, from 0.0016 to 0.26 M$_\odot$ (Hamuy 2003). The V-band photometry of SN 2004A in the nebular phase is converted to the bolometric luminosity using the bolometric correction of 0.26$\pm$0.06 mag derived from data on SN 1987A and SN 1999em (Hamuy 2003) and the distance and reddening estimated in the previous sections. The mass of ^{56}Ni was then found using equation (2) of Hamuy (2003) for each point in the nebular part of the lightcurve. A simple average of these estimates gives $M_{Ni} = 0.034 \pm 0.01 M_\odot$. The error was calculated in a standard manner. This method is strongly dependent on the explosion epoch, extinction and the distance used. Although the explosion epoch could be constrained well using the lightcurve of other type IIP supernovae, there is a large uncertainty associated with distance, and hence the large error.

6.3 Nickel mass from the 'steepness of decline' correlation

An alternative way of estimating mass of ^{56}Ni was suggested by Elmhamdi et al. (2003a). This method uses the rate of decline in the V band light curve from plateau to the nebular phase. Using a sample of type IIP supernovae Elmhamdi et al. (2003a) arrived at a

correlation between the rate of decline in the V band from the plateau to the tail phase and the mass of ^{56}Ni produced during the explosion. The supernovae having steeper decline during the transition are found to produce less amount of ^{56}Ni. The advantage with this method is that it is independent of distance and explosion epoch. A good coverage of data points during the transition from plateau to the nebular phase allowed us to estimate the steepness parameter accurately as $S = 0.1 \pm 0.007$. Hendry et al. (2006) have reexamined the correlation of Elmhamdi et al. (2003a) and provided improved co-efficients. With the improved relation the mass of ^{56}Ni is found to be $0.035 \pm 0.01 M_{\odot}$, which agrees very well with the mass of ^{56}Ni derived using the V magnitude on the radioactive tail.

A simple comparison of the bolometric luminosity in the radioactive tail of SN 2004A with that of SN 1987A also gives an approximate estimate of the mass of ^{56}Ni produced during the explosion with the assumption that the degree of deposition of γ-ray is the same for both the objects. The tail bolometric luminosity of SN 2004A is found to be fainter by 0.45 mag as compared to SN 1987A during the same epoch. Using mass of ^{56}Ni for SN 1987A as 0.075 M$_{\odot}$ (Turatto et al. 1998) the difference of 0.45 mag in the bolometric curve implies that 0.027 ± 0.01 M$_{\odot}$ of ^{56}Ni was produced during the explosion. A simple average of the three estimates gives the mass of ^{56}Ni produced as 0.032 ± 0.02 M$_{\odot}$.

7.   Estimation of physical parameters of the progenitor

Arnett (1980) first derived the analytic solutions for light curves of SNe IIP for the purpose to derive physical parameters. Litvinova & Nadyozhin (1985) used hydroynamical modelling to derive approximate relations between observable quantities, namely, the duration of the plateau, the absolute luminosity, and the photospheric velocity observed in the middle of the plateau and the physical parameters of the supernova explosion such as explosion energy E, mass of the envelope M, and the progenitor radius R. These equations provide a simple and quick method to derive E, M, R without going into the details of specific models. Recently, Hamuy (2003) applied these methods to obtain the physical parameters of 13 SNe IIP.

We applied these methods to SN 2004A, to estimate the explosion energy E, ejected envelope mass M, and the progenitor radius R. The observed parameters for SN 2004A namely, length of the plateau is estimated as 80 ± 5 days using the date of explosion and the V band light curve, the photospheric velocity at the mid of the plateau was estimated using the weak iron lines as $V_{ph} = 3300 \pm 250$ km s^{-1} and the absolute V magnitude Mv is -15.83$\pm$0.47. Using these parameters the explosion energy E, ejected envelope mass M, and the progenitor radius R are $4.7 \pm 2.7 \times 10^{50}$ ergs, 7.2 ± 2.2 M$_{\odot}$ and 199.7 ± 92.3 R$_{\odot}$, respectively. Assuming that the compact remnant has mass in the range a $\sim$ 2–3 M$_{\odot}$ we expect the mass of the progenitor before explosion to be $\sim 10 \pm 2.5$ M$_{\odot}$.

Hendry et al. (2006) have identified the progenitor of SN 2004A in a pre-explosion HST image at a magnitude of $m_{F814W} = 24.3\pm0.3$. They concluded that the progenitor of SN 2004A is a red supergiant with spectral class G5 to M5 with an initial mass of $9^{+3}_{-2}M_\odot$. Our estimates of the initial mass and radius of the progenitor are consistent with those derived by Hendry et al. (2006).

8.   Summary

We have presented the $BVRI$ photometric and spectroscopic data of SN 2004A. The shape of the light curve as well as the spectral evolution indicate that it is Type IIP supernova. Our photometric and spectroscopic observations of SN 2004A provide good coverage of all the three phases namely, photospheric, transition from photospheric to nebular and nebular phase.

The late phase photometry indicates that the decline rate of light curve during $\sim$ $120 - 250$ d was similar to the ^{56}Co to ^{56}Fe radioactive decay. The spectra of SN 2004A in early phase shows strong emission dominated H$_\alpha$ line that is shallower than other type IIP supernovae. The P-Cygni profile of H$_\alpha$ and H$_\beta$ is composed of two components. The velocity evolution of SN 2004A is studied using the hydrogen balmer lines and weak iron lines and is found to be similar to other type IIP supernovae. The mass of ^{56}Ni synthesized during the explosion is estimated to be $0.032 \pm 0.02 \, M_\odot$. The brightness of the plateau, its duration and the expansion velocity of the supernova at the middle of the plateau is used to estimate the explosion energy as $E_{exp} = 4.70 \pm 2.7 \times 10^{50}$ ergs. The main-sequence mass of the progenitor is estimated to be $10 \pm 2.5 M_\odot$.

Acknowledgments

References

Arnett, W. D., 1980, ApJ, 237, 541
Baron, E., et al. 2000, ApJ, 545, 444
Bessell, M. S., Castelli, F., & Plez, B., 1998, A&A, 333, 231
Cappellaro, E., et al. 2005, A&A, 430, 83
Cardelli, J. A., Clayton, G. C., & Mathis J. S., 1989, ApJ, 345, 245
Eastman, R. G., & Krishner, R. P., 1989, ApJ, 347, 771

Eastman, R. G., Schmidt, B. P., & Kirshner, R., 1996, ApJ, 466, 911

Elmhamdi, A., Chugai, N. N., & Danziger, I. J., 2003a, *A&A*, 404, 1077

Elmhamdi, A., et al., 2003b, *MNRAS*, 338, 939

Hamuy, M., et al. 2001, ApJ, 558, 615

Hamuy, M., & Pinto, P. A., 2002, ApJL, 566, L63

Hamuy, M., 2003, ApJ, 582, 905

Hamuy, M., 2004, in IAU Coll. 192, Cosmic Explosions, Eds J. M. Marcaide, & K. W. Weiler,
        Heidelberg: Springer, 535

Haynes, M. P., et al., 1998, AJ, 115, 62

Heger, A., et al., 2003, ApJ, 591, 288

Hendry, M. A., et al., 2006, MNRAS, 369, 1303

Horne, K., 1986, PASP, 98, 609

Kawakita, H., & Kinugasa, K., 2004, IAUC, 8266, 2

Krishner, R. P., & Kwan, J., 1974, ApJ, 193, 27

Landolt, A. U., 1992, AJ, 104, 340

Leonard, D. C., et al., 2002, PASP, 114, 35

Leonard, D. C., et al., 2003, ApJ, 594, 247

Litvinova, I. Y., & Nadyozhin, D. K., 1985, Soviet Astronomy Letters, 11, 145

Mannucci, F., della Valle, M., Panagia, N., Cappellaro, E., Cresci, G., Maiolino, R., Petrosian,
        A., & Turatto, M., 2005, A&A, 433, 807

Munari, U., & Zwitter, T., 1997, A&A, 318, 269

Nugent, P., et al., 2006, ApJ, 645, 841

Pastorello, A., et al., 2006, MNRAS, 370, 1752

Patat, F., et al., 1994, A&A, 282, 731

Sahu, D. K., et al., 2006, MNRAS, 372, 1315

Schlegel, D. J., et al. 1998, ApJ, 500, 525

Schmidt, B. P., et al., 1994, ApJ, 432, 42

Smartt, S. J., et al., 2002, ApJ, 565, 1089

Suntzeff, N. B., & Bouchet, P., 1990, AJ, 99, 650

Turatto, M., et al. 1998, ApJ 498, 129

Turatto, M., Benetti, S., & Cappellaro, E., 2003, in Proc. ESO/MPA/MPE Workshop: From
        Twilight to highlight: The physics of supernovae, eds W. Hillebrandt & B. Leibundgut,
        Springer-Verlag, 200

Woosley, S. E., & Weaver, T. A., 1986, ARAA, 25, 205